

Model-independent determination of the gap function of nearly localized superconductors

Dušan Kavický,¹ František Herman,^{1,2} and Richard Hlubina¹

¹*Department of Experimental Physics, Comenius University, Mlynská Dolina F2, 842 48 Bratislava, Slovakia*

²*Institute for Theoretical Physics, ETH Zürich, CH-8093, Switzerland*

(Dated: May 29, 2022)

The gap function $\Delta(\omega)$ carries essential information on both, the pairing glue as well as the pair-breaking processes in a superconductor. Unfortunately, in nearly localized superconductors with a non-constant density of states in the normal state, the standard procedure for extraction of $\Delta(\omega)$ cannot be applied. Here, we introduce a model-independent method that makes it possible to extract $\Delta(\omega)$ also in this case. The feasibility of the procedure is demonstrated on the tunneling data for the disordered thin films of TiN. We find an unconventional feature of $\Delta(\omega)$ which suggests that the electrons in TiN are coupled to a very soft pair-breaking mode.

A prototypical example of a quantum phase transition is provided by the quantum breakdown of superconductivity (QBS) which may occur when a suitable external parameter is changed [1]. In the special case when the QBS is due to increasing disorder, which is the subject of this paper, there exist at least three mechanisms which can drive the transition: (i) Within the so-called fermionic scenario [2, 3], increasing disorder causes the effective electron-electron interaction to decrease. Moreover, quantum corrections which lead to a suppressed density of states in the normal state [4] further strengthen the QBS. (ii) Whatever causes the initial suppression of T_c , at some point the phase stiffness of the superconductor necessarily becomes small and the phase fluctuations may destroy superconductivity. This is the so-called bosonic scenario of the QBS [5, 6]. (iii) The single-particle wavefunctions become strongly inhomogeneous before undergoing Anderson localization. Theories emphasizing this aspect of the QBS are known as the "emergent-granularity" scenario [7, 8].

When the QBS occurs in homogeneously disordered systems, all three mechanisms are intertwined: (i) The relevance of the fermionic scenario is documented most convincingly by the recent observation of quantum corrections to optical conductivity up to at least ~ 4 eV [9]. (ii) The temperature dependence of the resistivity indicates that phase fluctuations definitely can not be neglected in such systems [10, 11]. (iii) The measured spatial modulations of the tunneling density of states strongly suggest that also "emergent granularity", i.e. electronic inhomogeneity in structurally effectively homogeneous systems does play a role [10, 11]. Unfortunately, the combined effect of changing interactions, phase fluctuations, and localization is presently not understood [1].

The scaling of T_c with the distance from the critical point, the gap-to- T_c ratio, the magnitude of the critical resistivity, etc., further help to identify the symptoms of the various mechanisms driving the QBS [1]. On the other hand, a comprehensive picture of the transition would be provided by the knowledge of the gap func-

tion $\Delta(\omega)$ which is known to carry information not only on the pairing glue [12], but also on the pair-breaking processes [13, 14] which occur in a superconductor.

In case of conventional superconductors $\Delta(\omega)$ can be routinely extracted from the tunneling data [12]. For nearly localized superconductors such data are in fact available from a series of recent papers [10, 11, 15], but all of them find that the superconducting feature in the density of states develops on top of a normal-state background with a non-constant density of states, presumably due to interaction-induced corrections [4, 16]. In such case the standard extraction procedure [12] is not applicable. The goal of this paper is to demonstrate that, provided also the normal-state density of states is known from experiment, the superconducting gap function can nevertheless be determined, and the proposed procedure does not rely on any particular microscopic model.

Interaction-induced corrections to the normal-state density of states are present only if the electron self-energy depends on the energy ε of the one-particle eigenstates of the dirty system [17–19]. On the other hand, in order to take into account the retarded phonon-mediated pairing interactions, it is necessary to include also the frequency ω dependence of the self-energy. Thus a generalized version of the Eliashberg theory with an ε - and ω -dependent electron self-energy is needed for nearly localized superconductors. Such a theory has in fact been developed long ago [20] and a model calculation of the superconducting density of states $N_s(\omega)$ in that formalism became available recently [21].

Here, instead of applying the Eliashberg theory to a specific model of the superconductor, we take a model-independent approach. We start by switching off the coupling of the electrons to the phonons. In that case the ε -dependence of the self-energy, caused by the weakly screened electron-electron interactions, leads to a normal-state density of states $N_0(\varepsilon)$ with a minimum close to the Fermi level [4]. We emphasize that we do not need to specify the functional form of $N_0(\varepsilon)$ and we do not even have to require that it is particle-hole symmetric. Next

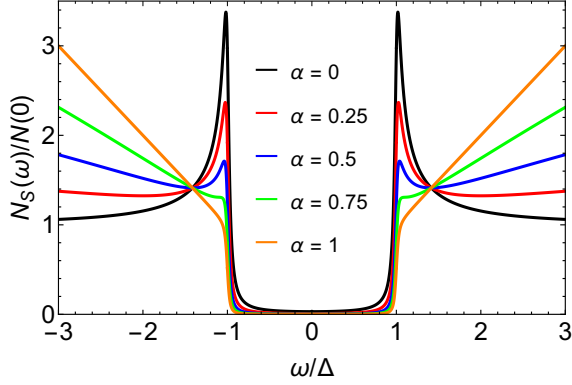


FIG. 1. Prediction of Eq. (2) for the superconducting density of states $N_s(\omega)$ of a Dynes superconductor with a small pair-breaking rate $\Gamma = 0.03 \Delta$. The normal-state density of states is described by the particle-hole symmetric model $N_n(\omega) = (|\omega|/\Delta)^\alpha N(0)$ with several values of the exponent α .

we switch the electron-phonon coupling on again and the observable density of states is found to be

$$N_i(\omega) = \int d\varepsilon N_0(\varepsilon) A_i(\varepsilon, \omega), \quad (1)$$

where $A_i(\varepsilon, \omega)$ is the spectral function of an electron in a one-particle eigenstate with energy ε . The index $i = n, s$ discriminates between the normal and superconducting states. In what follows it will be useful to split $N_i(\omega)$ into even and odd components, $N_i(\omega) = N_{ie}(\omega) + N_{io}(\omega)$, where $N_{ie}(-\omega) = N_{ie}(\omega)$ and $N_{io}(-\omega) = -N_{io}(\omega)$.

If we assume that the contribution of electron-phonon coupling to the electron self-energy depends just on the frequency ω as within the standard Eliashberg theory, then under reasonable assumptions we find the following approximate relations, see [22],

$$N_{se}(\omega) = \frac{d\Omega}{d\omega} N_{ne}(\Omega), \quad N_{so}(\omega) = N_{no}(\Omega). \quad (2)$$

The result Eq. (2) simply means that the density of states in the superconducting state at energy ω is determined by the normal-state density of states at a single ω -dependent energy $\Omega(\omega)$, to be determined later. Note that the factor $d\Omega/d\omega$ guarantees that the total number of states is the same in the normal and the superconducting states, since the odd part of the density of states does not contribute to the total number of states.

Moreover, we also find that, see [22],

$$\frac{d\Omega}{d\omega} = \text{Re} \frac{\omega}{\sqrt{\omega^2 - \Delta^2(\omega)}}, \quad (3)$$

where $\Delta(\omega)$ is the superconducting gap function [23]. This means that the function $d\Omega/d\omega = n(\omega)$, to be called the dos-function in what follows, plays the role of the density of states of a hypothetical superconductor with a constant density of states in the normal state.

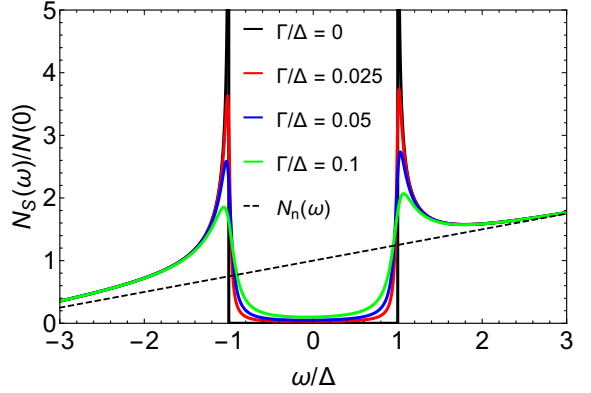


FIG. 2. Prediction of Eq. (2) for the superconducting density of states $N_s(\omega)$ of Dynes superconductors with several values of the pair-breaking rate Γ . The normal-state density of states $N_n(\omega)$, which is not particle-hole symmetric, is shown by the dashed line.

Let us investigate how $N_s(\omega)$ described by Eq. (2) depends on the form of $N_n(\omega)$. We assume the Dynes form of $\Omega(\omega) = \text{Re} \sqrt{(\omega + i\Gamma)^2 - \Delta^2}$ [14, 23], which implies that $n(\omega) = \text{Re}[(\omega + i\Gamma)/\sqrt{(\omega + i\Gamma)^2 - \Delta^2}]$. In Fig. 1 we show $N_s(\omega)$ calculated for a simple particle-hole symmetric model of the normal state $N_n(\omega) = (|\omega|/\Delta)^\alpha N(0)$ and several values of α . Note that while the apparent gap essentially does not depend on α , the magnitude of the "coherence peaks" in the vicinity of $\pm\Delta$ quickly decreases with increasing α . This shows that the frequently observed spatially constant gap coexisting with spatially modulated coherence peaks (see, e.g., Fig. 3 in [10]) may be caused by the spatial modulation of $N_n(\omega)$. Also the suppressed coherence peaks do not necessarily imply the presence of localized Cooper pairs as is sometimes claimed [24]. In Fig. 2 we show that when the normal state is not particle-hole symmetric, the asymmetry of $N_s(\omega)$ is comparable to that of $N_n(\omega)$ at energies much larger than the gap, while inside the gap it is reduced.

Let us turn back to our main goal of extracting the gap function $\Delta(\omega)$ from experimental data. In the first step, regarding the even part of Eq. (2) as a first-order differential equation $d\Omega/d\omega = F(\omega, \Omega)$ for the function $\Omega = \Omega(\omega)$ with the initial condition $\Omega(0) = 0$, we shall determine $\Omega(\omega)$ and consequently also the dos-function $n(\omega)$. Of course, in order to determine the function $F(\omega, \Omega) = N_{se}(\omega)/N_{ne}(\Omega)$, both the normal and the superconducting densities of states will have to be known. In the second step, the function $\Delta(\omega)$ shall be determined from $n(\omega)$ using Eq. (3). In order to demonstrate the feasibility of this two-step procedure, in what follows it shall be applied to the data for a homogeneously disordered thin film of TiN reported in Fig. 12 of [10]. Our crucial assumption, supported by Fig. 2 of that paper, is that the non-trivial form of $N_n(\omega)$ is due to normal-state corrections and not superconducting fluctuations.

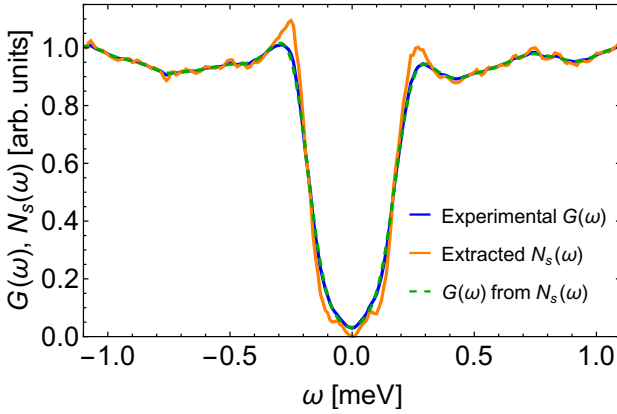


FIG. 3. Superconducting density of states $N_s(\omega)$ extracted from the differential conductance $G(\omega)$ of TiN measured at $T = 0.3$ K, see Fig. 12 of [10]. Second-order integral expansion has been used, see [22]. The dashed green line shows that the differential conductance obtained by plugging the extracted $N_s(\omega)$ into Eq. (4) perfectly matches the original data.

One should first realize that what is actually measured in experiments at a finite temperature T is the differential conductance $G(\omega)$, which (when appropriately normalized) is related to the density of states $N(\omega)$ by the integral expression

$$G(\omega) = \int d\omega' K(\omega' - \omega) N(\omega'), \quad (4)$$

where the kernel $K(\nu) = [4T \cosh^2(\nu/(2T))]^{-1}$ acts as a filter which suppresses the fine structure present in $N(\omega)$ on scales $\omega \lesssim T$. In the limit of vanishing temperature the kernel reduces to a delta-function and $N(\omega) = G(\omega)$. When the finite value of T can not be neglected, $N(\omega)$ is typically determined from the measured $G(\omega)$ by a fitting procedure: one postulates a functional form of $N(\omega)$ which depends on several parameters - typically two of them when fitting to the Dynes formula - and optimizes the values of the parameters.

However, this approach can not be applied in cases when we do not know the actual functional form of $N(\omega)$, which is precisely our case. Thus we need to solve the inverse problem of determining $N(\omega)$ from the measured $G(\omega)$ without recourse to fitting. We have tried several approaches, see [22], and the general features of the results which we find are pretty obvious: in convex (concave) regions of $G(\omega)$, the extracted density of states $N(\omega)$ lies below (above) the $G(\omega)$ data. As can be seen in Fig. 3, when the inversion procedure is applied to actual experimental data, the superconducting features in $N(\omega)$ are therefore more pronounced when compared with the bare $G(\omega)$ data. Note that for the same reason also noise-like features are amplified, but their magnitude in the example shown in Fig. 3 is seen to be still acceptable. The extraction of the normal-state density of states from Fig. 12 of [10] is described in detail in [22].

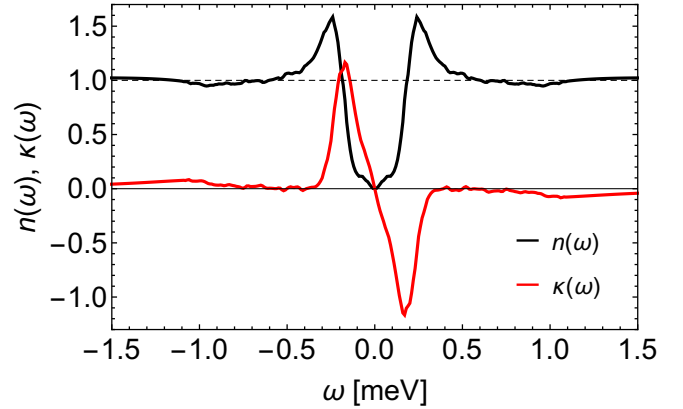


FIG. 4. The dos-function $n(\omega)$ determined by solving the symmetric part of Eq. (2). $N_{se}(\omega)$ is determined by symmetrization of the data from Fig. 3 and $N_{ne}(\omega)$ is taken from Fig. 7 in [22]. The relative normalization of $N_{se}(\omega)$ and $N_{ne}(\omega)$ has been determined as described in the text. The high-energy prolongation by $n(\omega) = 1 + a/\omega^2 + b/\omega^4$ with $a \approx 0.120$ meV² and $b \approx -0.156$ meV⁴ is plotted as well. Also shown is $\kappa(\omega)$, the Kramers-Kronig partner of $n(\omega)$.

Having $N_s(\omega)$ and $N_n(\omega)$ at our disposal, it is a straightforward exercise to determine the function $\Omega = \Omega(\omega)$ by solving the differential equation $d\Omega/d\omega = F(\omega, \Omega)$ implied by Eq. (2). The only subtle point has to do with the fact that tunneling determines the density of states only up to a multiplicative constant, and therefore the relative normalization of the functions $N_{se}(\omega)$ and $N_{ne}(\omega)$ is unknown in general. These two functions should merge in the limit of energies which are much larger than the superconducting gap, but since experimental data is available from [10] only up to $|\omega| = \Lambda = 1.1$ meV, a different procedure has to be used instead.

In this work, the relative norm of $N_{se}(\omega)$ and $N_{ne}(\omega)$ is chosen so that the resulting dos-function $n(\omega) = d\Omega/d\omega$ satisfies the constraint

$$\int_{-\infty}^{\infty} d\omega [n(\omega) - 1] = 0, \quad (5)$$

which requires that the superconducting transition conserves the total number of states. Moreover, this constraint guarantees that, as ω increases, the difference between $\Omega(\omega)$ and ω vanishes.

In order to estimate the contribution to the integral in Eq. (5) of the region $|\omega| > \Lambda$ where no data is available, in this region we assume that $n(\omega) = 1 + a/\omega^2 + b/\omega^4$. The two fitting parameters a and b are determined by requiring (i) that $n(\omega)$ is continuous at $\omega = \Lambda$, and (ii) that the constraint Eq. (5) is satisfied. It turns out that a and b can be found in a finite range of relative normalizations of the functions $N_{se}(\omega)$ and $N_{ne}(\omega)$, see [22]. The optimal normalization is then chosen by requiring that also the derivative of $n(\omega)$ is continuous at $\omega = \Lambda$.

The resulting dos-function $n(\omega)$ is plotted in Fig. 4. It looks much more BCS-like than the density of states

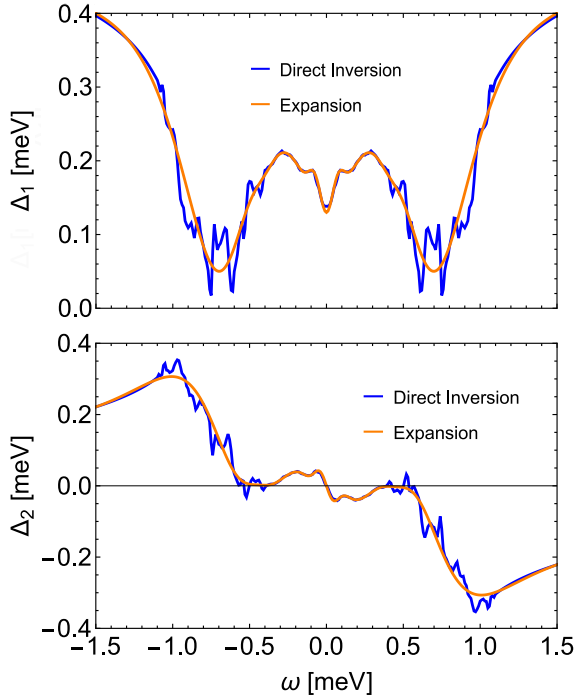


FIG. 5. Real and imaginary parts of the gap function extracted from the dos-function plotted in Fig. 4. Blue (orange) line: result of the direct inversion (inversion by expansion with $N = 11$ and $E = 0.45$ meV), see [22].

$N_s(\omega)$ shown in Fig. 3. In particular, the coherence peaks are substantially amplified. A surprising feature of the extracted dos-function $n(\omega)$ is the presence of broad local minima at $|\omega| = \omega_* \approx 1$ meV. This is a robust feature which is present in a finite range of relative normalizations of $N_{se}(\omega)$ and $N_{ne}(\omega)$, see [22].

Our next goal is to invert Eq. (3) and to determine the complex gap function $\Delta(\omega) = \Delta_1(\omega) + i\Delta_2(\omega)$ from the dos-function $n(\omega)$. We assume that $\Delta(-\omega) = \Delta^*(\omega)$ as in the standard Eliashberg theory, although we emphasize that the self-consistent Born approximation on which the Eliashberg theory is based might not be sufficient to describe the nearly localized superconductors [25].

We extract the gap function $\Delta(\omega)$ by a procedure proposed in [26], slightly modified for the case of gapless superconductors. Namely, we view the dos-function $n(\omega)$ as the real part of a complex function $n(\omega) + i\kappa(\omega)$ which, when continued to the upper half-plane of complex frequencies, is analytic and satisfies the Kramers-Kronig relations on the real axis. Therefore the imaginary part $\kappa(\omega)$ can be easily found by integration and the result is shown in Fig. 4. The complex gap function $\Delta(\omega)$ is then obtained (up to an overall sign) from the expression

$$\Delta^2(\omega) = \omega^2 [1 - 1/(n + i\kappa)^2]. \quad (6)$$

The result of this procedure, where the complex dos-function is taken from Fig. 4, is shown in Fig. 5. There we also plot $\Delta(\omega)$ with reduced noise which has been found

by expansion in a basis of rational eigenfunctions of the Hilbert transform, for details see [22].

We find that at low energies $\omega \lesssim 0.2$ meV, the gap function of the studied TiN sample is given by $\Delta(\omega) \approx \Delta_0 - i\Gamma\Delta_D/(\omega + i\Gamma)$, where $\Delta_0 \approx 0.19$ meV, $\Delta_D \approx 0.06$ meV, and $\Gamma \approx 0.05$ meV. However, in the low-energy limit the pair-breaking processes should cause the gap function to exhibit the Dynes form, and therefore we should find $\Delta_D = \Delta_0$ [14, 27]. The finite difference between Δ_D and Δ_0 which we observe might be caused by the subtleties of the extraction procedure of $N_s(\omega)$ from $G(\omega)$ at low energies, see [22], and therefore we do not draw any conclusions from this observation. Further work is definitely needed to clarify this issue.

At energies above the gap, two robust qualitative features of $\Delta(\omega)$ are present for all acceptable relative norms of $N_{se}(\omega)$ and $N_{ne}(\omega)$, see Fig. 5 and [22]: (i) a steep increase of $\Delta_1(\omega)$ around $\omega_* \approx 1$ meV and (ii) a concomitant sharp negative peak of $\Delta_2(\omega)$ at the same energy. A model calculation shows that these two features are a direct consequence of the local minimum of $n(\omega)$ close to ω_* , which in turn is caused by the unusual suppression of $N_s(\omega)$ with respect to $N_n(\omega)$ at energies above the gap, see [22]. When interpreted within the extended Eliashberg theory, the features (i) and (ii) of $\Delta(\omega)$ are consistent with a finite coupling of the electrons to a soft pair-breaking mode at ω_* , see Fig. 1b in [13].

The nature of the pair-breaking mode in TiN is unclear at present and it could be due to either of the three mechanisms for the QBS. Further insight should come, e.g., from the scaling of ω_* with the distance x from the critical point. We speculate that the already soft scale ω_* softens further as x decreases and ultimately vanishes at the critical point. This speculation can be tested by studying a set of samples with varying x . In addition, further measurements in a broader energy range and in more finely sampled magnetic fields, both achievable with current instrumentation, should substantially eliminate the uncertainties of the present analysis.

In conclusion, we have demonstrated that it is possible to extract the gap function $\Delta(\omega)$ of a superconductor, even if the normal-state density of states exhibits complicated structure due to quantum corrections. Our procedure requires that the tunneling conductance is known in both, the normal and the superconducting states, and in a sufficiently broad range of energies. When it is applied to available data for dirty TiN thin films [10], an indication of the coupling of the electrons to a very soft pair-breaking mode at approximately 1 meV is found. The coupling to this mode of currently unknown nature might be the ultimate killer of superconductivity.

This work was supported by the Slovak Research and Development Agency under Contract No. APVV-19-0371, by the VEGA Agency under Contract No. 1/0640/20, and by the Comenius University under Contract No. UK/343/2021.

Derivation of Eqs. (2,3) from the main text

Within the standard Eliashberg theory, the superconducting state is fully described by two complex functions of energy: the wavefunction renormalization $Z(\omega)$ and the gap function $\Delta(\omega)$. For future convenience it is useful to parametrize these functions by the four real functions of frequency $\tilde{\omega}(\omega)$, $\tilde{\gamma}(\omega)$, $\tilde{\Omega}(\omega)$, and $\tilde{\Gamma}(\omega)$, defined as follows:

$$Z(\omega)\omega = \tilde{\omega} + i\tilde{\gamma},$$

$$Z(\omega)\sqrt{\omega^2 - \Delta^2(\omega)} = \tilde{\Omega} + i\tilde{\Gamma}.$$

As in the main text, the branch of the square root is chosen in such a way that the sign of $\tilde{\Omega}$ is the same as the sign of ω . Furthermore we assume that, with this sign convention, $\tilde{\Gamma} > 0$. As will become clear soon, $\tilde{\Omega}$ is the energy of the quasiparticle in the superconducting state and Γ is its lifetime. The quantities $\tilde{\omega}$ and $\tilde{\gamma}$ have a similar but less transparent meaning.

Let us also introduce the following notation for a Lorentzian with width $\tilde{\Gamma}$:

$$\delta_{\tilde{\Gamma}}(x) = \frac{1}{\pi} \frac{\tilde{\Gamma}}{x^2 + \tilde{\Gamma}^2}.$$

In Appendix C of [28] it has been shown that the spectral function of a general Eliashberg superconductor, when viewed as a function of energy ε at fixed frequency ω , takes the following simple form

$$A_s(\varepsilon, \omega) = P\delta_{\tilde{\Gamma}}(\varepsilon - \tilde{\Omega}) + Q\delta_{\tilde{\Gamma}}(\varepsilon + \tilde{\Omega})$$

$$+ R\frac{4\pi\tilde{\Omega}^2}{\tilde{\Gamma}}\delta_{\tilde{\Gamma}}(\varepsilon - \tilde{\Omega})\delta_{\tilde{\Gamma}}(\varepsilon + \tilde{\Omega}), \quad (7)$$

where the ω -dependent weights of the three terms are

$$P = \frac{1}{2} \left(\frac{\tilde{\gamma}}{\tilde{\Gamma}} + 1 \right), \quad Q = \frac{1}{2} \left(\frac{\tilde{\gamma}}{\tilde{\Gamma}} - 1 \right), \quad R = \frac{1}{2} \left(\frac{\tilde{\omega}}{\tilde{\Omega}} - \frac{\tilde{\gamma}}{\tilde{\Gamma}} \right).$$

In what follows, the product of the two Lorentzians which appears in Eq. (7) will be approximated by the function

$$\delta_{\tilde{\Gamma}}(\varepsilon - \tilde{\Omega})\delta_{\tilde{\Gamma}}(\varepsilon + \tilde{\Omega}) \approx \frac{1}{4\pi} \frac{\tilde{\Gamma}}{\tilde{\Omega}^2 + \tilde{\Gamma}^2} \left[\delta_{\tilde{\Gamma}}(\varepsilon - \tilde{\Omega}) + \delta_{\tilde{\Gamma}}(\varepsilon + \tilde{\Omega}) \right].$$

Note that the areas under the curves of ε on both sides of this approximate equality are the same for all ratios of $\tilde{\Omega}$ and $\tilde{\Gamma}$. As pointed out in [28], the approximation is very good in the case when $\tilde{\Omega} \gg \tilde{\Gamma}$. In the opposite case $\tilde{\Omega} \ll \tilde{\Gamma}$ the approximation is still reasonable, although not perfect.

Plugging this approximation into Eq. (7), after some algebra we find a simplified expression for the spectral function

$$A_s(\varepsilon, \omega) = \frac{1}{2} [n(\omega) + 1] \delta_{\tilde{\Gamma}}(\varepsilon - \tilde{\Omega}) + \frac{1}{2} [n(\omega) - 1] \delta_{\tilde{\Gamma}}(\varepsilon + \tilde{\Omega}),$$

according to which the spectral function consists of just two Lorentzians with weights determined by the dos-function

$$n(\omega) = \text{Re} \left[\frac{\tilde{\omega} + i\tilde{\gamma}}{\tilde{\Omega} + i\tilde{\Gamma}} \right] = \text{Re} \frac{\omega}{\sqrt{\omega^2 - \Delta^2(\omega)}}.$$

Now let us insert the simplified spectral function into the defining Eq. (1) for the density of states. If we take into account that the width of the Lorentzians is $\tilde{\Gamma}$, we find immediately that

$$N_s(\omega) = \frac{1}{2} [n(\omega) + 1] \bar{N}_0(\tilde{\Omega}) + \frac{1}{2} [n(\omega) - 1] \bar{N}_0(-\tilde{\Omega}),$$

where $\bar{N}_0(\varepsilon)$ is an appropriately smoothed version of the auxiliary function $N_0(\varepsilon)$.

More formally, the above expression for $N_s(\omega)$ can be obtained as follows. First, let us introduce an analytic function $\mathcal{N}(z)$ in the upper half-plane of complex energy z whose real part reduces to the function $N_0(\varepsilon)$ at the real axis, $\text{Re}[\mathcal{N}(\varepsilon + i0)] = N_0(\varepsilon)$. Next we complete the ε integral in Eq. (1) by a semicircle at infinity in the upper half-plane, obtaining a closed path C . Since $A_s(z, \omega) \propto z^{-2}$ at the semicircle, Eq. (1) can be rewritten as

$$N_s(\omega) = \text{Re} \int_C dz \mathcal{N}(z) A_s(z, \omega).$$

Making use of the residue theorem one can check readily that our expression for $N_s(\omega)$ is valid and $\bar{N}_0(\varepsilon)$ can be calculated as $\bar{N}_0(\varepsilon) = \mathcal{N}(\varepsilon + i\tilde{\Gamma})$.

The same set of arguments applied to the normal state would lead to the expression $N_n(\omega) = \bar{N}_0(\tilde{\omega})$, since $n(\omega) = 1$ in this case. Strictly speaking, in the normal state the width of the Lorentzians is $\tilde{\gamma}$ and not $\tilde{\Gamma}$ as in the superconducting state, and therefore we should introduce two different functions $\bar{N}_0(\varepsilon)$ for the normal and superconducting states. However, in what follows we will neglect this difference.

Finally, in the low-energy limit (with respect to the phonon energy) we can write $\tilde{\omega} \approx (1 + \lambda)\omega$ where λ is the electron-phonon coupling constant. Therefore the auxiliary function $\bar{N}_0(\omega)$ can be expressed in terms of the observable density of states in the normal state, $N_n(\omega)$, as $\bar{N}_0(\omega) = N_n(\frac{\omega}{1 + \lambda})$. Making use of this expression, the result for $N_s(\omega)$ can be finally written as

$$N_s(\omega) = n(\omega)N_{ne}(\Omega) + N_{no}(\Omega), \quad (8)$$

where $\Omega = \tilde{\Omega}/(1 + \lambda)$ and we have split the function $N_n(\varepsilon)$ into even and odd parts $N_{ne}(\varepsilon)$ and $N_{no}(\varepsilon)$.

But once it is established that the superconducting density of states at energy ω depends on the normal-state density of states at energy Ω via Eq. (8), the conservation of the total number of states implies that $n(\omega) = d\Omega/d\omega$ must hold. This completes the justification of Eqs. (2,3) from the main text. An a posteriori check of the quality of our approximations will be presented later and the results are presented in Fig. 15.

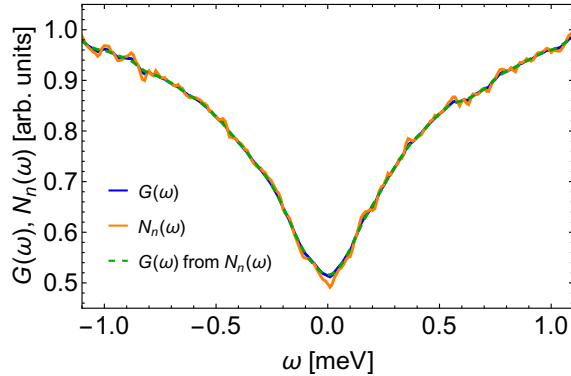


FIG. 6. Density of states $N_n(\omega)$ extracted from the differential conductance $G(\omega)$ of TiN measured at $T = 0.3$ K in the field of 4 T, see Fig. 12 of [10]. Second-order integral expansion has been used. The dashed green line shows that the differential conductance obtained by plugging the extracted $N_n(\omega)$ into Eq. (4) perfectly matches the original data.

Extraction of $N(\omega)$ from the tunneling conductance

When discretized, Eq. (4) can be written symbolically as $G = KN$. Therefore the formal solution to this equation reads $N = K^{-1}G$. However, the matrix K is nearly singular so that its inversion is numerically unstable. Singular value decomposition does reduce the noise in the output, but we find it difficult to find good balance between the noise level in N and the quality of the solution $\|KN - G\|$. Standard maximum entropy inversion (with a constant prior) does perform better, but the same problem (although reduced) still persists.

We find that at low (but non-negligible) temperatures which are of interest here the following method works best. We can always write $K = 1 + D$, where D is the deviation of the operator K from identity. The crucial observation is that, at low temperatures, D is small. Therefore the inverse operator K^{-1} can be expressed as $K^{-1} = (1 + D)^{-1} = 1 - D + D^2 + \dots$. Since the action of $D = K - 1$ corresponds to a simple integration, we can easily compute the sequence $N^{(n)}$ of approximants to N , namely $N^{(0)} = G$, $N^{(1)} = (1 - D)G$, $N^{(2)} = (1 - D + D^2)G$, and so on.

The quality of these approximants can be tested by the deviation $\delta^{(n)} = \|KN^{(n)} - G\|$ between the prediction $KN^{(n)}$ of the approximant for the conductivity and the measured conductivity G , and one can easily show that $\delta^{(n)} = \|D^n G\|$. Therefore, at small D , the quality of the solutions quickly improves with n . However, similarly as was the case with other methods, also the noise increases with n and we have chosen to work with $n = 2$, see Fig. 3.

For the sake of completeness, in Fig. 6 we show the result of the inversion procedure for the normal state. As was to be expected, the deviation of the density of states N from the conductance G is very small in this case and we have decided to ignore it.

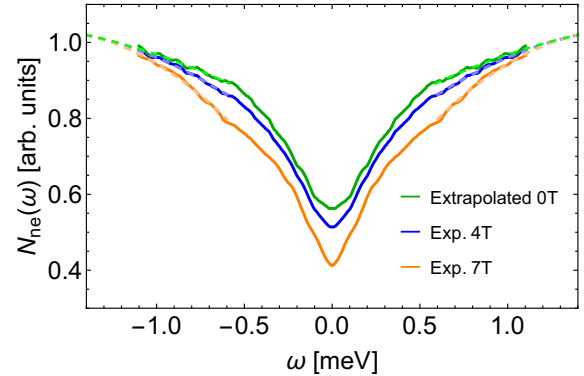


FIG. 7. Even part of the normal-state density of states (in arbitrary units) extrapolated from the data for 4 T and 7 T in Fig. 12 of [10] to $B = 0$ T. Dashed lines show smooth extrapolations of the measured data which merge at ≈ 1.4 meV.

We should note that our integral expansion method does not guarantee that the extracted density of states N is positive definite. In the normal state this does not cause problems, see Fig. 6, but in the superconducting state the extracted density of states becomes slightly negative in the vicinity of $\omega = 0$. Whenever this happens, we set $N(\omega) = 0$. Fortunately, as shown in Fig. 3, in our case this procedure does not spoil the agreement between $KN^{(2)}$ and G . However, the pathologies of $\Delta(\omega)$ observed in Fig. 5 in the immediate vicinity of $\omega = 0$ might be caused by this problem.

There exists yet another problem which arises when we extract the normal-state density of states from the data in Fig. 12 of [10]. Namely, the normal-state data is magnetic field-dependent, but what we need is the extrapolation of the data to $B = 0$ T.

In order to solve this problem, we are led by the observation made in [15] that the normal-state data for MoC films in different fields merge at an energy of the order of $2\mu_B B$. In the first step, assuming that the same physics applies also to the TiN films studied in [10], we choose the relative normalization of the normal-state data in 4 T and 7 T in such a way that their smooth extrapolations merge at an energy outside the measured window, see Fig. 7. In the next step, assuming furthermore that $N_n(\omega, B) = N_n(\omega, 0) + a(\omega)B^2$, we obtain an estimate of the $B = 0$ density of states $N_n(\omega, 0)$ from the appropriately normalized 4 T and 7 T data, which were obtained in the first step. The result of this procedure for the even part of $N_n(\omega, 0)$ is shown in Fig. 7.

Relative norm of $N_{se}(\omega)$ and $N_{ne}(\omega)$.

As mentioned in the main text, there is some freedom in choosing the normalization of the normal-state density of states $N_{ne}(\omega)$, if the norm of the superconducting density of states $N_{se}(\omega)$ is kept fixed. In Fig. 8 we show

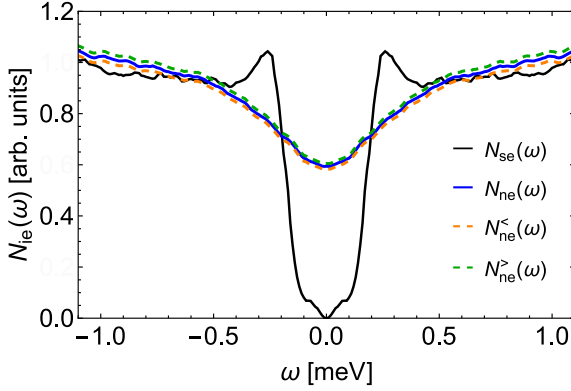


FIG. 8. The optimal choice $N_{ne}(\omega)$ of the normal-state density of states together with two extremal acceptable choices $N_{ne}^{<}(\omega)$ and $N_{ne}^{>}(\omega)$, see text. The norm of the superconducting density of states $N_{se}(\omega)$ is kept fixed.

three normalizations of $N_{ne}(\omega)$, all of which generate dos-functions $n(\omega)$ which satisfy the constraint Eq. (5) and are continuous at $|\omega| = \Lambda$. The optimal choice called $N_{ne}(\omega)$ in Fig. 8 leads to a solution where also the derivative $dn(\omega)/d\omega$ is smooth at $|\omega| = \Lambda$, whereas the choices $N_{ne}^{<}(\omega)$ and $N_{ne}^{>}(\omega)$ correspond to extremal solutions where the discontinuity of $dn(\omega)/d\omega$ at $|\omega| = \Lambda$ is still acceptable.

The three dos-functions $n(\omega)$, $n^{<}(\omega)$, and $n^{>}(\omega)$ extracted from the three normalizations $N_{ne}(\omega)$, $N_{ne}^{<}(\omega)$, and $N_{ne}^{>}(\omega)$ are shown in Fig. 9. The inset shows how the numerically determined dos-functions for $\omega < \Lambda$ merge with their prolongations to $\omega > \Lambda$. Note that the function $n(\omega)$ is essentially smooth at $\omega = \Lambda$, while $n^{<}(\omega)$ and $n^{>}(\omega)$ exhibit small upward and downward kinks, respectively. The coefficients describing the prolongations are

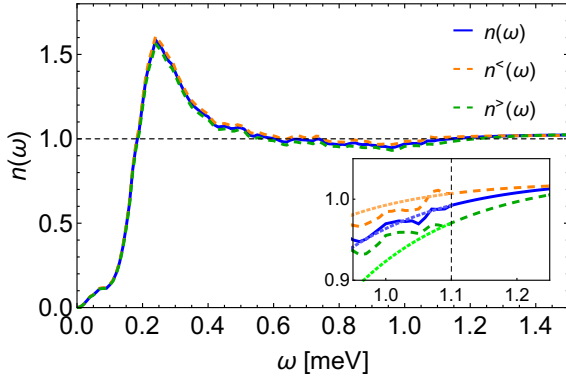


FIG. 9. The optimal dos-function $n(\omega)$ and two extremal acceptable dos-functions $n^{<}(\omega)$ and $n^{>}(\omega)$ corresponding to the choices $N_{ne}(\omega)$, $N_{ne}^{<}(\omega)$, and $N_{ne}^{>}(\omega)$ from Fig. 8. Only the $\omega > 0$ part of these even functions is plotted. The inset shows the dos-functions in the vicinity of the energy $\omega = \Lambda = 1.1$ meV (indicated by the vertical dashed line). For energies $\omega < \Lambda$ where data extracted from experiments are available, the prolongations $1 + a/\omega^2 + b/\omega^4$ are shown by dotted lines.

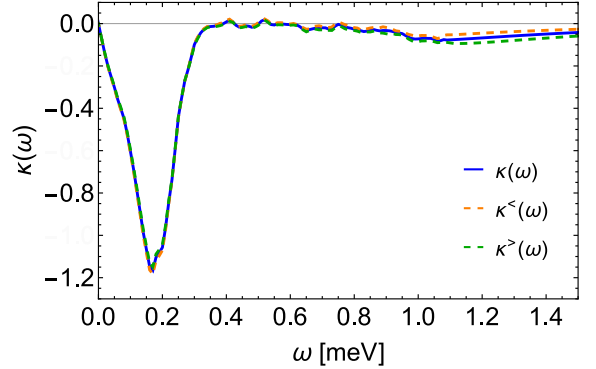


FIG. 10. The Kramers-Kronig partners $\kappa(\omega)$ of the three dos-functions $n(\omega)$ from Fig. 9. Only the $\omega > 0$ part of these odd functions is plotted.

$a \approx 0.084$ meV 2 and $b \approx -0.091$ meV 4 for $n^{<}(\omega)$ and $a \approx 0.160$ meV 2 and $b \approx -0.236$ meV 4 for $n^{>}(\omega)$.

The imaginary part of the complex dos-function $n(\omega) + i\kappa(\omega)$, shown in Fig. 10, is calculated by using the Kramers-Kronig relations making use of the three sets of data for $n(\omega)$ from Fig. 9. Remarkably, all $\kappa(\omega)$ curves look quite BCS-like and they exhibit a weak structure in the vicinity of $\omega_* \approx 1$ meV, where $n(\omega)$ exhibits a minimum. Thanks to Eq. (5), at large energies the functions $\kappa(\omega)$ decay as ω^{-3} . We have also checked that, starting from $\kappa(\omega)$ and applying the Kramers-Kronig relations in the reverse direction, we do reproduce the dos-functions $n(\omega) - 1$.

Extraction of $\Delta(\omega)$ from $n(\omega) + i\kappa(\omega)$

Model gap function. Before carrying out the full numerical calculation of $\Delta(\omega)$ from $n(\omega) + i\kappa(\omega)$, we would like to point out that both main qualitative deviations of the observed complex dos-function from the BCS prediction, i.e. the local minimum of $n(\omega)$ at $\omega \approx \omega_*$ and the negative peak (for $\omega > 0$) of $\kappa(\omega)$ at the same energy, can be explained by a simple model gap function $\Delta(\omega)$.

In fact, let us assume that the real part of the gap function is similar to a simple two-value function, $\Delta_1(\omega) \approx \Delta_0$ for $|\omega| < \omega_*$ and $\Delta_1(\omega) \approx \Delta_\infty$ for $|\omega| > \omega_*$, where Δ_0 is smaller than Δ_∞ . Making use of the results of [29], a smooth complex function with these properties can be found, which satisfies also the Kramers-Kronig relations. The result reads as

$$\Delta(\omega) = \Delta_\infty + (\Delta_0 - \Delta_\infty) F(\omega), \quad (9)$$

$$F(\omega) = \frac{i}{\pi} \left[\Psi \left(\frac{1}{2} + \frac{\omega + \omega_*}{2\pi i \Theta} \right) - \Psi \left(\frac{1}{2} + \frac{\omega - \omega_*}{2\pi i \Theta} \right) \right],$$

where $\Psi(z)$ is the digamma function and Θ measures the width of the transition regions around $|\omega| = \omega_*$. As shown in Fig. 11, this model gap function does produce the qualitative features of the measured dos-function

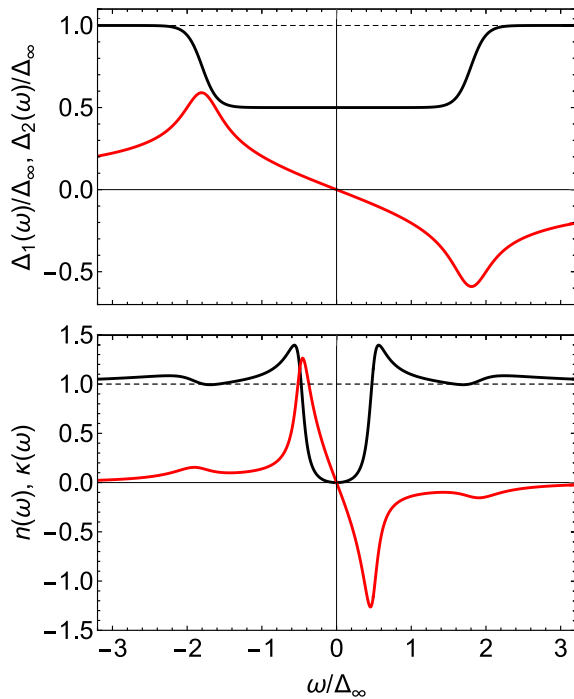


FIG. 11. Upper panel: the model gap function $\Delta(\omega)$ described by Eq. (9) for $\Delta_0/\Delta_\infty = 0.5$, $\omega_*/\Delta_\infty = 1.8$, and $\Theta/\Delta_\infty = 0.1$. Lower panel: the complex dos-function implied by this $\Delta(\omega)$. In both panels, the black (red) lines correspond to the real (imaginary) parts of the functions.

$n(\omega) + i\kappa(\omega)$. Thus we should expect that the numerical solution exhibits some similarity to the model Eq. (9).

Direct extraction. Let us proceed with the full numerical extraction of $\Delta(\omega)$. As explained in the main text, if at a given frequency both $n(\omega)$ and $\kappa(\omega)$ are known, then $\Delta(\omega)$ can be found from Eq. (6). However, at a fixed frequency ω , the complex number $\Delta(\omega)$ is known only up to an overall sign. The potentially troublesome point is that the choice of signs at two different frequencies is completely independent of each other.

Fortunately, in regions where the absolute value $|\Delta(\omega)|$ is large, this does not cause any problems. In fact, having fixed the signs of Δ_1 and Δ_2 at some frequency, due to the expected continuity of $\Delta(\omega)$ we have to take the same sign convention also at the neighboring frequency. Problems therefore arise only in regions where $|\Delta(\omega)|$ is small, because in these regions continuity does not tell us how to match the sign conventions at neighboring frequencies. Thus, if such regions are present, then we are not guaranteed that the function $\Delta(\omega)$ is reconstructed correctly.

There does exist a tool, however, which makes it possible to decide whether the signs have been chosen correctly. Namely, the complex function $\Delta(\omega)$ should obey the Kramers-Kronig relations. We have checked that our choice of signs does satisfy these relations.

It is worth pointing out in passing that, when calcu-

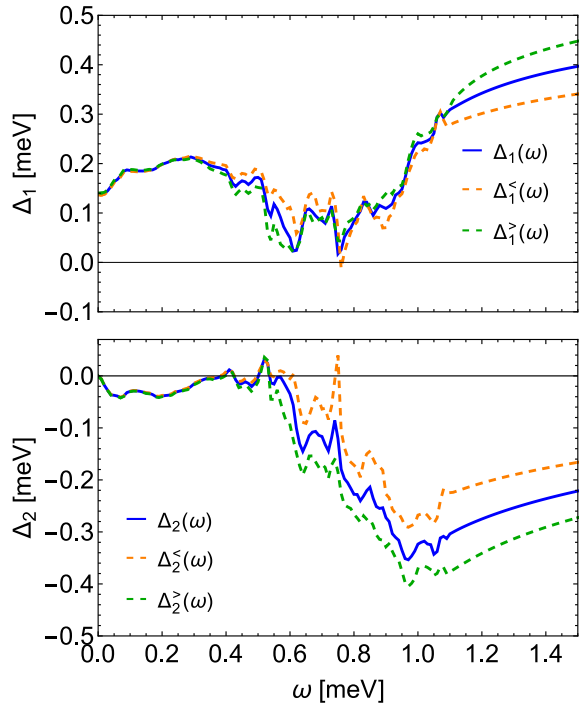


FIG. 12. Real and imaginary parts of the gap functions extracted, using Eq. (6), from the dos-functions plotted in Figs. 9 and 10. The same color coding has been used as in Fig. 9. Only the $\omega > 0$ part of the functions is shown.

lating $\Delta_1(\omega)$ from $\Delta_2(\omega)$ using the Kramers-Kronig relations, we had to add by hand the asymptotic value of $\Delta_\infty = \sqrt{2a}$ implied by the functional form of the prolongation of $n(\omega)$ to large frequencies. For completeness let us also add that at high energies $\Delta_2(\omega) \propto \omega^{-1}$ which is consistent with $\kappa(\omega) \propto \omega^{-3}$.

In Fig. 12 we show the results of a direct extraction of the gap functions from the complex dos-functions plotted in Figs. 9 and 10. Note that up to ≈ 0.3 meV the gap functions are essentially independent of the relative norm of $N_{se}(\omega)$ and $N_{ne}(\omega)$ for all acceptable values of this norm, but also at higher energies the qualitative features are the same in all solutions: a steep rise of $\Delta_1(\omega)$ and a negative peak of $\Delta_2(\omega)$, both taking place around $\omega = \omega_*$. These are precisely the features of the simple model gap function Eq. (9), as expected.

Extraction by expansion. As is obvious from the comparison of Figs. 9 and 10 with Fig. 12, the direct extraction of $\Delta(\omega)$ using Eq. (6) strongly amplifies the noise which is inevitably present in the dos-function. Therefore an alternative method for the extraction of $\Delta(\omega)$ is required which does not suffer from this problem. Unfortunately, a simple smoothing of $\Delta_1(\omega)$ and $\Delta_2(\omega)$ does not solve the problem, since the result would not be guaranteed to satisfy the Kramers-Kronig relations.

Instead, we make use of an expansion of the gap func-

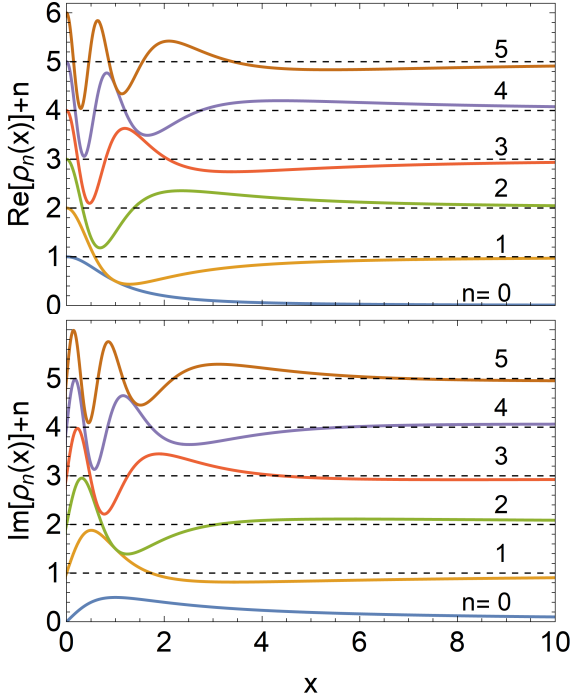


FIG. 13. Real (upper panel) and imaginary (lower panel) parts of the basis functions $\rho_n(x)$ for $n = 0, \dots, 5$. Note that, with increasing n , the period of oscillations at small x increases and, at the same time, the largest nodes x_n of both components grow.

tion in terms of the rational functions [30]

$$\rho_n(x) = \frac{(1+ix)^n}{(1-ix)^{n+1}}, \quad n = 0, \pm 1, \pm 2, \dots,$$

which form a complete basis in the space of complex square-integrable functions on the real axis. The functions $\rho_n(x)$ satisfy the orthogonality relations

$$\int_{-\infty}^{\infty} \rho_n^*(x) \rho_m(x) = \pi \delta_{nm},$$

which imply that the coefficients in the expansion of the function $f(x) = \sum_n a_n \rho_n(x)$ can be calculated as

$$a_n = \frac{1}{\pi} \int_{-\infty}^{\infty} dx \rho_n^*(x) f(x).$$

The first few functions $\rho_n(x)$ are shown in Fig. 13.

The crucial point to observe is that $\rho_n(x)$ are eigenfunctions of the Hilbert transform, i.e. they satisfy

$$\frac{1}{\pi} P \int_{-\infty}^{\infty} \frac{dx \rho_n(x)}{x-y} = i \text{sgn}(n) \rho_n(y),$$

where $P \int dx$ denotes the principal value integration [30].

Making use of the relations $\rho_{-n-1}(x) = \rho_n^*(x) = \rho_n(-x)$ and of the symmetry $\Delta(-\omega) = \Delta^*(\omega)$ we then

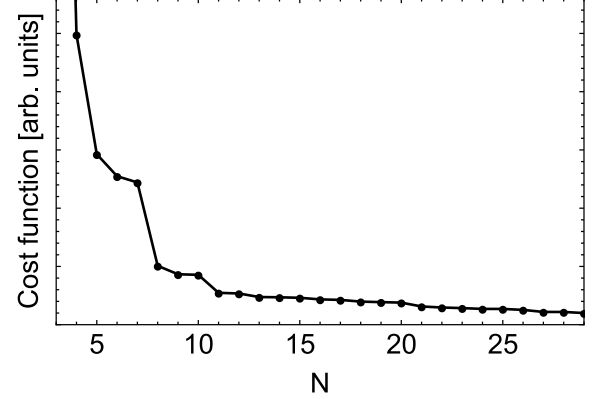


FIG. 14. Dependence of the cost function on the order N of the expansion for $E = 0.45$ meV.

find that the gap function can be written as

$$\Delta(\omega) = \Delta_{\infty} + 2 \sum_{n=0}^{\infty} a_n \rho_n \left(\frac{\omega}{E} \right), \quad (10)$$

where E is an arbitrary energy scale and a_n are real coefficients. One can check readily that the gap function given by Eq. (10) is analytic in the upper half-plane and satisfies the Kramers-Kronig relations.

The coefficients a_n for $n = 0, 1, \dots, N$ which appear in Eq. (10) are determined by minimization of the following cost function. At small energies $|\omega| < \Lambda$ the cost function is given by the distance between the measured complex dos-function and $n(\omega) + i\kappa(\omega)$ calculated from Eq. (10) using Eq. (6). At large energies $|\omega| > \Lambda$ the cost function is given by the distance between Eq. (10) and the directly determined gap function $\Delta(\omega)$, since the latter is not any more noisy in the large-energy region. The described choice of the cost function is dictated by the fact that at large energies, the complex dos-function is a very weak function of $\Delta(\omega)$.

The energy scale E which appears in Eq. (10) can be chosen arbitrarily. With the aim to keep the order of the expansion N small, we take $E = 0.45$ meV. In order to fix the optimal value of N for this choice of E , we study how the cost function varies with N . The result of this calculation is shown in Fig. 14. As expected, the cost function decreases monotonically with N . Moreover, in the limit of large N the cost function should vanish, because in that limit Eq. (10) reproduces exactly the direct solution.

What we are after is a solution with the least possible N which does reproduce faithfully the measured complex dos-function. Based on Fig. 14, we have chosen to take $N = 11$, since the decay of the cost function for $N > 11$ is slow, indicating that inclusion of further basis functions in the expansion Eq. (10) improves only the agreement with noise-like features in $n(\omega) + i\kappa(\omega)$.

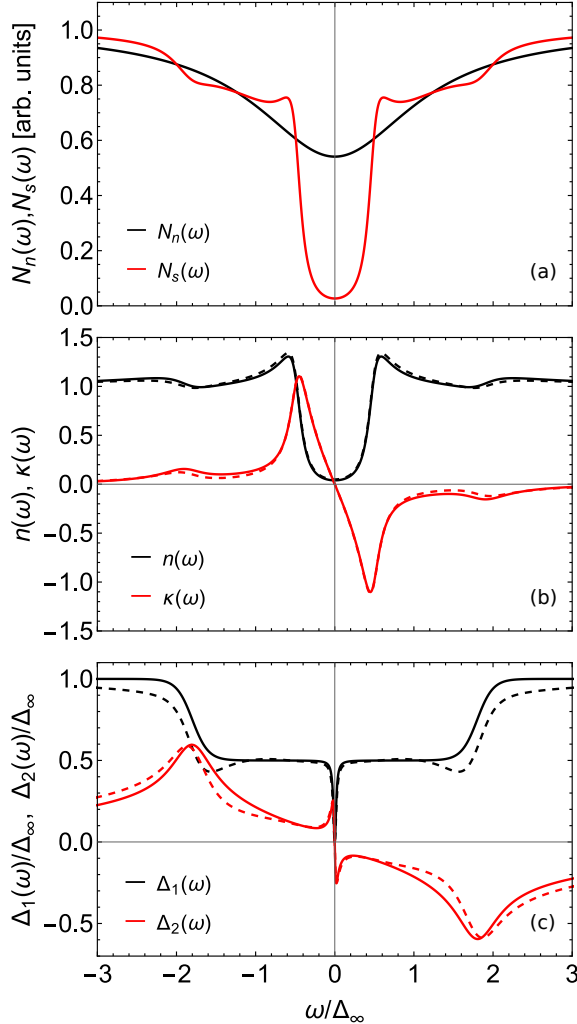


FIG. 15. Test of the inversion procedure using model data, see text for more details. The auxiliary function $N_0(\varepsilon)$ is parametrized by $\alpha/\Delta_\infty = 1.76$ and $V/\Delta_\infty = 1.2$. The gap function is parametrized by $\Delta_0/\Delta_\infty = 0.5$, $\omega_*/\Delta_\infty = 1.8$, $\Theta/\Delta_\infty = 0.1$, and $\Gamma/\Delta_\infty = 0.02$. (a): exact densities of states in the normal and superconducting states, $N_n(\omega)$ and $N_s(\omega)$. (b): exact (solid) and extracted (dashed) dos-functions $n(\omega) + i\kappa(\omega)$. (c): exact (solid) and extracted (dashed) gap functions $\Delta(\omega)$.

Test of the extraction procedure

Our analysis is based on Eqs. (2,3) which are valid only approximately. In order to check the quality of our procedure, finally we perform the following test with parameters chosen so as to resemble the experimental data.

We consider a conductor with a suppressed density of states in the vicinity of the Fermi level, described by a model auxiliary function $N_0(\varepsilon) \propto 1 - \alpha\delta_V(\varepsilon)$. The parameters α and V measure the depth and the width of the suppression, respectively.

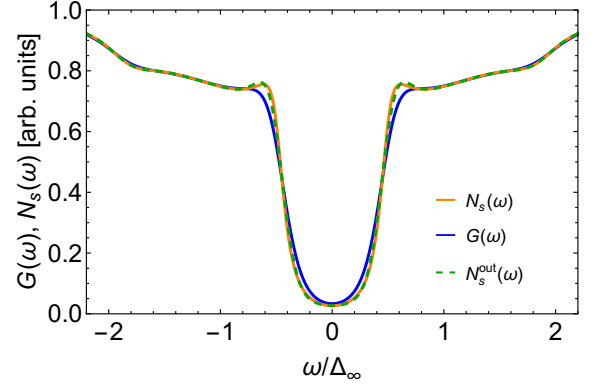


FIG. 16. Test of the inversion of the tunneling data. The differential conductance $G(\omega)$ has been determined from the input density of states $N_s(\omega)$ at temperature $T = 0.054\Delta_\infty$. $N_s^{\text{out}}(\omega)$ was extracted from $G(\omega)$ by second-order integral expansion.

For the gap function of the superconductor, we take

$$\Delta(\omega) = \Delta_\infty + (\Delta_0 - \Delta_\infty)F(\omega) - \frac{i\Gamma\Delta_D}{\omega + i\Gamma}.$$

The first two terms reproduce the gap function Eq. (9) characterized by two gap values Δ_0 and Δ_∞ , with a crossover between the two characterized by its position ω_* and width Θ . In order to compare with experiment, we have to take $\Delta_\infty \approx 0.49$ meV, as required by the prolongation parameter $a \approx 0.12$ meV². The last term, in which we take $\Delta_D = \Delta_\infty + (\Delta_0 - \Delta_\infty)F(0) \approx \Delta_0$, generates at low energy a Dynes-like feature in $\Delta(\omega)$ characterized by the parameter Γ . Also for the wavefunction renormalization we take a Dynes-like expression $Z(\omega) = 1 + i\Gamma/\omega$.

Making use of the functions $N_0(\varepsilon)$, $\Delta(\omega)$, and $Z(\omega)$ in Eqs. (1,7), we calculate the exact densities of states in the normal and superconducting states, $N_n(\omega)$ and $N_s(\omega)$. The results are shown in panel (a) of Fig. 15.

Next, applying the numerical inversion procedure based on Eqs. (2,3) and taking $N_n(\omega)$ and $N_s(\omega)$ as input data, we determine the function $\Omega = \Omega(\omega)$ and, consequently, also the complex dos-function $n(\omega) + i\kappa(\omega)$. In panel (b) of Fig. 15 we compare our result with the exact dos-function calculated directly from the gap function $\Delta(\omega)$ using Eq. (3). Note that the agreement of our procedure with the exact data is very good.

Finally, from the complex dos-function we extract the gap function using Eq. (6). In panel (c) of Fig. 15, the result of this extraction is compared with the original gap function $\Delta(\omega)$. One can observe that, while the agreement is not perfect, all features of the gap function are reproduced correctly. This completes our test of Eqs. (2,3).

For the sake of completeness, let us also test the procedure for the extraction of the density of states from the thermally smeared tunneling data $G(\omega)$. To this end, we start by assuming that the superconducting density of

states $N_s(\omega)$ introduced in Fig. 15 is exact and, taking it as input, we calculate $G(\omega)$ at the experimental temperature $T = 0.054\Delta_\infty$. Next, taking $G(\omega)$ as input, we extract the density of states $N_s^{\text{out}}(\omega)$ by second-order integral expansion. The result is plotted in Fig. 16. We find that the difference between $N_s^{\text{out}}(\omega)$ and $N_s(\omega)$ is very small. Hence it is sufficient to stop the expansion at second order.

To conclude let us mention that we have also investigated the combined effect of the steps tested separately in Figs. 15 and 16. Namely, we have started the computation with the model data for the finite-temperature conductivities, extracted the densities of states, and afterwards performed the inversion procedure. The results were essentially identical to those reported in Fig. 15.

[1] B. Sacépé, M. Feigel'man, and T. M. Klapwijk, *Nat. Phys.* **16**, 734 (2020).

[2] P. W. Anderson, K. A. Muttalib, and T. V. Ramakrishnan, *Phys. Rev. B* **28**, 117 (1983).

[3] For a review, see A. M. Finkelstein, *Physica B* **197**, 636 (1994).

[4] B. L. Altshuler and A. G. Aronov, *Solid State Commun.* **30**, 115 (1979).

[5] S. Doniach, *Phys. Rev. B* **24**, 5063 (1981).

[6] M. P. A. Fisher, *Phys. Rev. Lett.* **65**, 923 (1990).

[7] M. Ma and P. A. Lee, *Phys. Rev. B* **32**, 5658 (1985).

[8] M. V. Feigelman, L. B. Ioffe, V. E. Kravtsov, and E. Cuevas, *Ann. Phys.* **325**, 1390 (2010).

[9] P. Neilinger, J. Greguš, D. Manca, B. Grančič, M. Kopčík, P. Szabó, P. Samuely, R. Hlubina, and M. Grajcar, *Phys. Rev. B* **100**, 241106(R) (2019).

[10] S. V. Postolova, A. Yu. Mironov, V. Barrena, J. Benito-Llorens, J. G. Rodrigo, H. Suderow, M. R. Baklanov, T. I. Baturina, and V. M. Vinokur, *Phys. Rev. Research* **2**, 033307 (2020).

[11] C. Carbillet, V. Cherkez, M. A. Skvortsov, M. V. Feigel'man, F. Debontridder, L. B. Ioffe, V. S. Stolyarov, K. Ilin, M. Siegel, D. Roditchev, T. Cren, and C. Brun, *Phys. Rev. B* **102**, 024504 (2020).

[12] W. L. McMillan and J. M. Rowell, *Phys. Rev. Lett.* **14**, 108 (1965).

[13] T. Bzdušek and R. Hlubina, *Philosophical Magazine* **95**, 609 (2015).

[14] See D. Kavický and R. Hlubina, *Phys. Rev. B* **102**, 014508 (2020), and references therein.

[15] M. Žemlička, M. Kopčík, P. Szabó, T. Samuely, J. Kačmarčík, P. Neilinger, M. Grajcar, and P. Samuely, *Phys. Rev. B* **102**, 180508(R) (2020).

[16] It should be pointed out that there exist also extrinsic causes of a nontrivial background, most notably the energy dependence of the tunneling matrix element. In STM experiments, such effects can be safely excluded if the tunneling spectra do not depend on the tip-sample distance, for a review see Ø. Fischer et al., *Rev. Mod. Phys.* **79**, 353 (2007).

[17] G. Rickayzen, *Green's Functions and Condensed Matter* (Academic, London, 1980).

[18] W. L. McMillan, *Phys. Rev. B* **24**, 2739 (1981).

[19] This statement does not apply at strong coupling when the interaction strength exceeds the bandwidth.

[20] D. Belitz, *Phys. Rev. B* **40**, 111 (1989) and references therein.

[21] B. Rabatin and R. Hlubina, *Phys. Rev. B* **98**, 184519 (2018).

[22] See Supplemental Material at [URL will be inserted by publisher] for additional details, which includes Refs. [28]-[30].

[23] The branch of the square root is chosen so that the sign of the square root is the same as the sign of ω .

[24] B. Sacépé, T. Dubouchet, C. Chapelier, M. Sanquer, M. Ovadia, D. Shahar, M. Feigel'man, and L. Ioffe, *Nature Phys.* **7**, 239 (2011).

[25] An explicit example where the self-consistent Born approximation is insufficient is provided by the Dynes superconductors [14].

[26] A. A. Galkin, A. I. D'yachenko, and V. M. Svistunov, *Sov. Phys. JETP* **39**, 1115 (1974).

[27] A. A. Mikhailovsky, S. V. Shulga, A. E. Karakozov, O. V. Dolgov, and E. G. Maksimov, *Solid State Commun.* **80**, 511 (1991).

[28] F. Herman and R. Hlubina, *Phys. Rev. B* **95**, 094514 (2017).

[29] G. Bevilacqua, G. Menichetti, and G. Pastori Parravicini, *Eur. Phys. J. B*, **89**, 3 (2016).

[30] J. A. C. Weideman, *Mathematics of Computation* **64**, 745 (1995).